Compensating regime in axisymmetric vortical flows

A.Y. KLIMENKO
The University of Queensland
School of Engineering
St.Lucia, Qld 4072
AUSTRALIA

Abstract: Axisymmetric vortices with high level of axial vorticity are considered. Consistency conditions result in so-called compensating regime of the vortical flow. The power laws associated with this regime are applied to a series of vortices of different scales: bathtub vortex, tornadoes and tropical cyclones.

Key–Words: vortical flows, bathtub vortex, tornado, tropical cyclone

1 Introduction

This work considers features that are common for bathtub-type vortical flows. These flows are characterized by a converging motion which can dramatically amplify the rotation present in the flow. Even if the initial intensity of rotation is so small that it remains virtually undetected (like, for example, the Earth rotation), the amplification may result in formation of the vortex near the axis of the flow with visible and even intense rotation. In order to achieve significant amplification of rotational components of velocity, the fluid particles have to reduce their distance from the axis by a very large factor. This relatively simple general scheme of formation of the vortex is valid for phenomena of very different scales: starting from the vortex in a bathtub and finishing with tornados and cyclones [1]. The region, where the amplification of rotation takes place, can be referred to as the intensification region. Although different vortices represent distinctly different phenomena, some degree of similarity can be expected in the intensification region which is characterized by prime importance of convective evolution of the vorticity.

Simple observations of the bathtub vortices indicate that vortical flows are axisymmetric, inviscid, mostly laminar and nearly steady. These features of vortical flows should be interpreted with caution since, for axisymmetric steady and inviscid flows, the directions of vorticity and velocity must coincide. In the present, work we identify a regime that is based on consistent level of tangential vorticity production and compensates for possible variations of surrounding conditions. This regime, which is termed here as "compensating", can under certain conditions be approximated by power laws. Applicability of these power laws to the vortices of different scales is one of the issues discussed in the present work.

2 Equations governing axisymmetric vortical flows

The normalized system of equations governing axisymmetric incompressible flows with vorticity can be written in the form

$$L_*^2\frac{\partial^2\Psi}{\partial Z^2}+R\frac{\partial}{\partial R}\left(\frac{1}{R}\frac{\partial\Psi}{\partial R}\right)=-R\Omega_\theta \qquad (1)$$

$$\frac{D\Omega_\theta/R}{DT}=-2K_*^2\frac{\Gamma\Omega_r}{R^3}+\frac{(...)}{\mathrm{Re}_*} \qquad (2)$$

$$\Omega_\theta=L_*^2\frac{\partial V_r}{\partial Z}-\frac{\partial V_z}{\partial R},\quad \frac{D\Gamma}{DT}=\frac{(...)}{\mathrm{Re}_*} \qquad (3)$$

where

$$\frac{D}{DT}\equiv \mathrm{St}_*\frac{\partial}{\partial T}+V_z\frac{\partial}{\partial Z}+V_r\frac{\partial}{\partial R} \qquad (4)$$

$$V_z=\frac{1}{R}\frac{\partial\Psi}{\partial R},\quad V_r=-\frac{1}{R}\frac{\partial\Psi}{\partial Z} \qquad (5)$$

$$\Omega_r=-\frac{1}{\mathrm{St}_*}\frac{1}{R}\frac{\partial\Gamma}{\partial Z};\quad \Omega_z=\frac{1}{\mathrm{St}_*}\frac{1}{R}\frac{\partial\Gamma}{\partial R} \qquad (6)$$

and the dimensionless parameters — the Reynolds number, the Strouhal number, the rotation vorticity number and the geometrical parameter — are introduced as

$$\mathrm{Re}_*=\frac{L_*v_*r_*}{\nu},\quad \mathrm{St}_*=\frac{r_*^2\omega_*}{\gamma_*}=\frac{r_*}{t_*v_*L_*},$$

$$K_*=\frac{(\gamma_*\omega_*)^{1/2}}{v_*},\quad L_*\equiv\frac{r_*}{z_*} \qquad (7)$$

The viscous terms are shown by dots in (1)-(3). The cylindrical coordinates z, r, θ, the velocities v_z, v_r, v_θ the vorticity ω_z, ω_r, ω_θ, the stream function ψ and the circulation $\gamma = v_\theta r$ are normalized according to

$$R = \frac{r}{r_*},\ Z = \frac{z}{r_*/L_*},\ V_r = \frac{v_r}{v_* L_*},\ V_z = \frac{v_z}{v_*},$$

$$\Psi = \frac{\psi}{\psi_*},\ \Omega_\theta = \omega_\theta \frac{r_*}{v_*},\ T = \frac{t}{t_*},\ t_* = \frac{\gamma_*}{\omega_* v_* r_* L_*},$$

$$v_* = \frac{\psi_*}{r_*^2},\ \Gamma = \frac{\gamma}{\gamma_*},\ \Omega_z = \frac{\omega_z}{\omega_*},\ \Omega_r = \frac{\omega_r}{\omega_* L_*} \quad (8)$$

The characteristic values and parameters based on these values are indicated by asterisk. The other conventional parameters — the swirl ratio, the Ekman number and the Rossby number — are linked to K_*, Re_* and St_* by the equations

$$S_* \equiv \frac{\gamma_*}{v_* r_*} = \frac{K_*}{\mathrm{St}_*^{1/2}},\quad \mathrm{Ek}_* \equiv \frac{\nu r_*^2}{z_*^2 \gamma_*} = \frac{L_*^3}{\mathrm{Re}_* S_*},$$

$$\mathrm{Ro}_* \equiv \frac{v_*}{r_* \omega_*} = \frac{1}{K_* \mathrm{St}_*^{1/2}} \quad (9)$$

The rotational vorticity parameter $K_* = (S_*/\mathrm{Ro}_*)^{1/2}$ represents a geometrical average of the swirl ratio and the inverse Rossby number. The parameter K_* determines the rate of generation of tangential vorticity Ω_θ by equation (2). If K_* is small and rotation in a bathtub-type flow remains relatively weak, then its complete description is easy: the flow on the planes passing through the axis must be close to potential (the term potential is used here to indicate that $\Omega_\theta \approx 0$). We, of course, are interested in a relatively fast rotation in the flow, whose description is far from being trivial. The case of large K_* and strong rotation in the flow, which we call the strong vortex approximation, was considered in Refs. [2, 3, 4]. The analysis originated in Refs. [5, 6, 7] shows that the situation is more complicated and the strong vortex approximation should be applied with caution.

3 The compensating regime

It is reasonable to assume that the stream function can be represented in the intensification region by a power law $\Psi = C_0 R^\alpha Z$ with exponent α unknown a priori. This assumption is consistent with the overall expected structure of a bathtub-like flow, with the strong vortex approximation (for any α) and with the low-K_* case (potential flow with $\alpha = 2$ or $\alpha = 0$). The dimensional equations for the stream function ψ, velocity components v_z and v_r, tangential vorticity ω_θ and convergence λ are given by

$$\psi = c_0 r^\alpha z,\ v_r = -c_0 r^{\alpha-1},\ v_z = \alpha c_0 r^{\alpha-2} z,$$

$$\omega_\theta = \alpha(2-\alpha) c_0 r^{\alpha-3} z,\ \ \lambda \equiv -\frac{1}{r}\frac{\partial v_r r}{\partial r} = c_0 \alpha r^{\alpha-2} \quad (10)$$

The dimensionless form of these equations represents the leading order terms of the strong vortex approximation [6, 7]. The dimensional form used here is more convenient for our purposes. The values of α from the range $1 < \alpha \leq 2$ correspond to a bathtub-like flow where we expect that $v_z \nrightarrow 0$ as $r \to 0$ and $v_r \to 0$ as $r \to 0$. If viscous effects are neglected, the quasi-steady solutions for $\omega_z = \Omega_z \omega_*$ and $\omega_r = \Omega_r \omega_* L_*$ can be obtained by applying the operators $\partial/\partial r$ and $\partial/\partial z$ to the second equation in (3):

$$\omega_r = 0,\ \omega_z = \frac{-c_1}{r v_r} = \frac{c_1}{c_0 r^\alpha},\ \gamma = \gamma_0(t) + \gamma_1 \quad (11)$$

where

$$\gamma_1 \equiv \left\{ \begin{array}{ll} \frac{c_1}{c_0} \ln(r), & \alpha = 2 \\ \frac{c_1}{c_0(2-\alpha)} r^{2-\alpha}, & \alpha < 2 \end{array} \right\}$$

c_0 and c_1 are constant while γ is determined by integrating ω_z using equation (6). It is possible to demonstrate that, if $\alpha \neq 2$ in an inviscid flow, any initial distribution of the axial vorticity approaches to $\omega_z \sim r^{-\alpha}$ in the velocity field given by (10). We note that even if the axial vorticity dependence on r is given by a power law, the tangential velocity

$$v_\theta = \frac{\gamma}{r} = \frac{\gamma_0}{r} + \frac{c_2}{r^{\alpha-1}},\quad c_2 = \frac{c_1}{c_0(2-\alpha)} \quad (12)$$

is represented by a power law $v_\theta \sim 1/r^\beta$ only when one of the terms γ_0 or γ_1 dominates the other (note that $\alpha \neq 2$ in (12)).

Vortical flows usually have a sufficiently wide range of radii to create conditions for substantial amplification of axial vorticity. Since different radii r_* can be characterized by different characteristic values of the parameter K_*, we introduce the local value K defined in terms of local parameters by $K = (\gamma \omega_z)^{1/2}/v_z$. In principle, K may exhibit a strong dependence on r as specified by the equation

$$K^2 \equiv \frac{\gamma \omega_z}{v_z^2} = K_*^2 \frac{\Gamma \Omega_z}{V_z^2} \sim \frac{\gamma}{r^{3\alpha-4}} \quad (13)$$

One can expect that K should not become very large or very small in a developed bathtub-like flow. Indeed, if $K \to \infty$ as $r \to 0$, then no sufficient amount of the tangential vorticity can be generated near the axis and the flow must become potential ($\omega_\theta \approx 0$) there. This leads us to a contradiction since the potential flow corresponds to $\alpha = 2$ and, if $\alpha = 2$, K must increase towards the axis according to (13). If, on the contrary, $K \to \infty$ as $r \to 0$, then, on one hand, equation (13)

requires sufficiently large α while, on the other hand, the large magnitudes of tangential vorticity ω_θ generated by (2) would, according to (10), decrease α. Hence, we conclude that, in a developed vortical flow, parameter K should have the same order at different radii r. The condition $K \sim 1$ applied to (13) results in a power law when

$$\alpha^* = \left\{ \begin{array}{ll} 4/3, & \gamma_0 \gg \gamma_1 \\ 3/2, & \gamma_0 \ll \gamma_1 \end{array} \right\} \qquad (14)$$

In this equation, α^* denotes the value of α that ensures that $K \sim 1$. The exponent $\alpha = \alpha^*$ is defined to compensate for possible increases or decreases of K and we call this regime "the compensating regime" while the value α^* is referred to as the compensating exponent. The constants $4/3$ and $3/2$ represent two limiting values for the compensating exponent but, practically, when γ_0 and γ_1 have similar magnitudes, α^* can vary between the limiting values.

In general, K is likely to be small during the initial stage of the vortex formation since rotation is weak in this stage. This flow remains potential ($\omega_\theta \approx 0$) and this problem is, effectively, linear: evolution of the vorticity is determined by the velocity field but the vorticity ω_θ is not strong enough to affect the translational components of the velocity v_z and v_r. Linear behavior can also be observed at the final stages of the vortex existence when axial vorticity becomes exhausted around the vortex but the vortex still persists for some time due to the axial vorticity accumulated in the viscous core (note that $K = 0$ when $\omega_z = 0$ even if $\gamma > 0$). Here, we see a developed vortex as a non-linear phenomenon where evolution of vorticity does significantly affect the translational velocity components. The translational velocities in a linear vortex are fully controlled by the boundary conditions and the vortex can be easily destroyed by flow disturbances while the nonlinear vortex has a self-organizing structure that makes it more stable. Since $\alpha = 2$ in the linear vortex the convergence λ remains uniform while in a non-linear vortex $\alpha < 2$ and λ increases towards the axis.

The arguments that K can not be small in a developed vortex are offset by the arguments that K can not be very large. If $K \to \infty$ as $r \to 0$, the analysis of Ref. [6] demonstrates existence near the axis of a non-trivial disturbance that complies with the boundary condition and this indicates that the vortical flow is likely to bifurcate and loose stability. This situation can not be dismissed as totally unrealistic but it is not consistent with the concept of a stable and persistent vortex. Hence, we can use $K \sim 1$ as the first approximation and the power laws (14) are obtained from this estimation. On one hand, large values K correspond to the strong vortex approximation but nonlinear interactions of vorticity and velocity trigger a mechanism that prevents further K increases. It is probably easier to conclude that $K \sim 1$ than to explain the physical balancing mechanism that prevents very large and very small values of K. This mechanism is based on existence of a negative feedback between the value of exponent α and parameter K: decrease in K reduces ω_θ that increases α that increases K (and vise versa). In general, non-linear interactions of velocity and vorticity are known to be responsible for instabilities and turbulence but, in case of a bathtub-like vortices, these interactions appear to have some stabilizing effect. The physical mechanism behind this effect is considered in Refs. [5, 7].

4 Formation of the vortex

During the initial period of vortex formation, the axial vorticity level is, generally, low and K is uniformly small; hence this vortex can be treated as linear and $\alpha = 2$ in the vortex. As rotation is amplified K also increases. As soon as $K \sim 1$ is achieved in a certain region, the vortex becomes non-linear and changes structure to noticeable levels of ω_θ in this region. According to equation (2), this requires presence of the radial vorticity ω_r. A discussed in the following section, the mechanism of generating ω_r of "correct" sign may be different for different vortices but it is a fact that ω_θ, which amplifies λ towards the axis and stabilizes the updraft motion, is present in vortical flows. We expect in the non-linear region that α drops below 2 and the compensating regime prevents any further significant increase of K in this region. We distinguish two cases when initial distribution of the axial vorticity is 1)quasi-steady $\omega_z \sim 1/r^2$ and 2) uniform $\omega_z \sim \mathrm{const}$. In the first case, $K \sim 1$ is achieved first near the axis and the compensating regime then extends sidewise [7]. In the second case, which seems to be more relevant to formation of atmospheric vortices, $K \sim 1$ is achieved at the periphery and the compensating regime propagates towards the axis. The ring of compensating regime screens, to some extent, the inner disk from atmospheric disturbances allowing for the vortex formation. Although $\alpha = 2$ and the vortex is still linear within the disk, rotation there amplifies and the inner boundary of the compensating regime propagates towards the axis.

When the strong vortex is formed the value of γ_0 will continue to rise if no losses are encountered in the flow and, eventually, this vortex would loose its stability when K becomes excessively high. Practically, a positive value of γ_0 amplifies the losses due to very fast rotation near the axis. It seems that γ_0 remains small compared to γ_1 in many realistic vortices.

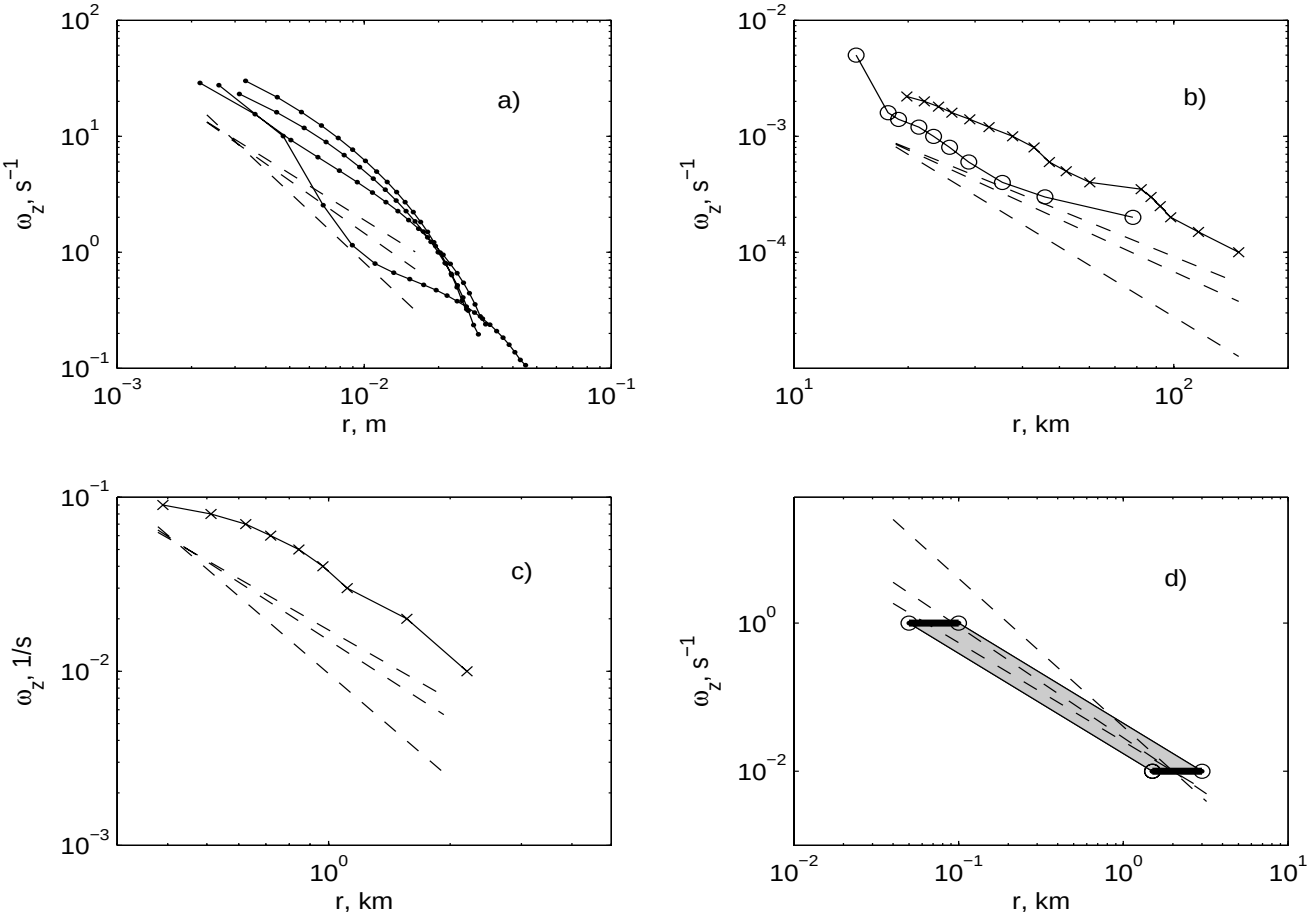

Figure 1: Dependence of axial vorticity on radius for different vortices: a) bathtub vortex [8], b) hurricanes Hilda (x) and Inez (o) [15, 16], c) tornado 4 of McLean storm [10] and d) typical characteristics of large supercell tornados [9, 10, 12]. In all figures, the dashed lines show three exponents of $\alpha = 2, 3/2$ and $4/3$ in $\omega_z \sim 1/r^{\alpha}$. The references point to sources of data used in evaluation of the curves.

5 Intensification region in different vortical flows

The intensification region is primarily characterized by amplification of rotation due to convective evolution of vorticity. This region does not have a characteristic radius on its own and, in real vortices, is bounded by a viscous core at the axis and by outer scales of the flow at the periphery of the vortex. The core is normally controlled by viscosity (molecular or turbulent) and, may be, buoyancy although, in some vortices, viscous core is replaced by a aircore. Detecting power laws within the intensification region requires a good separation of the inner and outer scales (which is not always the case in real vortices) and, for this purpose, one needs to select the strongest and most stable vortices. It should be also noted that, if axial vorticity is exhausted in surrounding flow, the vortex stream function can revert to $\psi \sim r^2 z$. As considered in (12), if the axial vorticity is given by the power law $\omega_z \sim 1/r^{\alpha}$, this does not necessarily mean that the tangential velocity is also represented by a power law $v_\theta \sim 1/r^{\beta}$ Hence, comparison of the power laws of the compensating regime with measurements using axial vorticity is more direct than that using tangential velocity.

5.1 Bathtub vortex

In a bathtub vortex, the inner boundary of the intensification region is determined by the size of the aircore while the outer scales are typically linked to the geometry of the tub. Even under conditions of potential flow, the drain located at the center of the flow creates conditions for generating ω_r of "correct" sign [7]. Shiraishi and Sato [8] measured experimental profiles of $v_\theta = \gamma/r$ for vortical flow in a bathtub. The reported curves $v_\theta(r)$ do not have a significant dependence on z and are sufficiently smooth to allow for numerical differentiation by polynomial approxima-

tions of the curves. The axial vorticity profiles are presented in Fig. 1a. The profile for the case of the smallest drain hole (20mm) and the weakest rotation in the flow appears to be less regular (the overall slope of the curve in this case seems to be closer to $\alpha = 2$) while the near axis asymptotes of $\omega_z(r)$ for other cases (the drains of 30, 40, and 50 mm) indicate α varying between 3/2 and 4/3. The exponent of $\alpha = 4/3$ was also observed in numerical simulations of a bathtub-like flow [7].

5.2 Tornadoes

The strongest and most stable tornadoes with intense rotation usually appear as a part of supercell thunderstorms. The maximal rotational speeds are achieved in the core of the tornado and then v_θ decreases with radius. Turbulent viscosity is deemed to be a determining factor in the core that makes distribution of axial vorticity more uniform. At its largest scales, the tornado is embedded into a mesocyclone whose characteristic scale is 10-40km [1]. At the scales of several kilometers, the air flow is affected by both the tornado and the core of the parent mesocyclone. The flow in mesocyclones involves more irregular components. Interactions of atmospheric flows with the earth surface result in atmospheric boundary layers. The interactions are most intense near the surface but extend to higher AGLs (levels above the ground) of several kilometers high. The boundary layer introduces ω_r into the flow (the Ekman effect).

We focus our attention on the intensification region which is intermediate between the core and mesocyclone scales. This region extends from the radius of few hundred meters to the radius of few kilometers with characteristic AGL of several hundred meters. According to Brooks et. al. [9], a supercell tornado amplifies the axial vorticity from $\sim 0.01\text{s}^{-1}$ in the area with a span of 3-7km to the level of $\sim 1\text{s}^{-1}$ in the core of the tornado. Dowell and Bluestein [10] summarized research on tornadoes available in other publication by stating that a tornado-producing storm amplifies the axial vorticity from $\sim 0.01\text{s}^{-1}$ in the region of a scale of ~ 5km to the level of $\sim 1\text{s}^{-1}$ in the core region with a scale of ~ 100m. On the basis of these data and other observations [12] we select the radii of 1.5-3.5km (the scale of 3-7km) for the outer tornadic vorticity of $\omega_z = 0.01\text{s}^{-1}$ in the core of the parent mesocyclone and the radii of 50-100m (the scale of 100-200m) for the tornadic core vorticity of $\omega_z = 1\text{s}^{-1}$. Figure 1d demonstrates that the power laws of $\alpha = 4/3$ and $\alpha = 3/2$ do not contradict the commonly accepted characteristics of supercell tornadoes. Wurman and Gill [11] presented high resolution measurements of a F4 tornado formed in a supercell storm near Dimmitt (Texas) in 1995 and reported a tangential velocity profile that can be approximated by $v_\theta \sim 1/r^\beta$ with $\beta = 0.6 \pm 0.1$ that corresponds to $\alpha = \beta + 1 = 1.6 \pm 0.1$. The value of $\alpha^* = 3/2$ is within this range.

Dowell and Bluestein [10] reported characteristics of several tornadoes that appeared in the 1995 McLean (Texas) storm based on Doppler radar measurements. Among these tornadoes, tornado 4, which reached F4-F5 on the Fujita scale, was the strongest, largest and most stable tornado with a relatively uniform distribution of the axial vorticity with height (which is consistent with the strong vortex approximation). The results are plotted in Fig. 1c. The curve has been determined from the contour plot of the constant values of vorticity by calculating the average effective radius of each contour line. The exponents of the compensating regime produce a good match to the measured vorticity within the range of $400\text{m} < r < 1.5\text{km}$.

5.3 Hurricanes

Tropical cyclones (hurricanes and typhoons) are the largest and most stable vortices observed in the Earth atmosphere [14, 13]. Compared to tornadoes, the flow pattern in tropical cyclones is more stable and the cyclones can persist for many days. Typically, stronger tropical cyclones, which affect weather on a large territory, are more symmetric and, thus, more interesting for us. The outer diameter of a strong cyclone can reach 500-1000km [13]. The core region of the cyclone is represented by the eye surrounded by the eye wall and has a characteristic radius of around 20-40km. This region has a noticeably higher temperature and is strongly affected by buoyancy while the temperature increments in surrounding flow are much smaller. The maximal wind speeds are achieved within the outer rim of the core. The intensification region, which still has significant winds and updrafts, extends from the radius of 20-40km to the radius of 130-250km. The region located outside the intensification region — the peripheral region — covers a large area with the radius of 500-1000km that is still subject to noticeable influence of the cyclone. The peripheral region can be approximately treated as a two-dimensional vortical sink without any significant updraft motion and the estimates of $\beta = 1$ are common for this region. Although $\beta = 0.5$ (corresponding to $\alpha = \beta + 1 = 3/2$) is considered to be the best average approximation in the intensification region [14, 13], particular measurements of the wind profiles in cyclones can have some scattering around this value. As in case of tornadoes, the Ekman effect is likely to be responsible for generation of ω_r in cyclones.

Detailed measurements of axial vorticity were reported for category 4 hurricanes Hilda (1964) and Inez (1966) [15, 16]. As expected, the temperature anomalies measured in these hurricanes were relatively small in what we call the intensification region but became much more significant in the eye. The profiles of angular momentum (i.e. circulation) and axial vorticity reported for Inez and Hilda (and also many other cyclones) appear to be independent of z up to the altitudes of at least two kilometers. The dependence of ω_z on r in hurricanes Hilda and Inez is shown in Fig. 1b. The values shown are taken from lower altitudes where ω_z does not depend on z. The slope of the curves $\omega_z \sim 1/r^\alpha$ exhibits some variations but is generally consistent with the lines of $\alpha = 3/2$ and $\alpha = 4/3$. At the radius of $r \sim 20$km, the Inez curve enters the eye wall and its slope becomes much steeper than in the intensification region $r > 20$km. This behavior can be explained by intensive generation of ω_θ by the substantial radial temperature gradients and by influence of turbulent transport which is expected to be more intensive in the core region.

6 Concluding remarks

The intensification region is an intermediate region that is limited by the core and peripheral scales and characterized by primarily convective amplification of axial vorticity. Existence of the intensification region is common for vortices of different nature (bathtub vortex, tornadoes, tropical cyclones). In the intensification region, the nonlinear interactions of velocity and vorticity have some stabilizing and self-organizing effect on the flow leading to the compensating regime: the developed vortical flow is constrained by balancing the tangential vorticity generation so that the rotational vorticity parameter K is neither very large nor very small. The compensating regime corresponds to an essentially vortical flow (i.e. $\omega_\theta \neq 0$) with $\alpha < 2$ and the flow convergence λ increasing towards the axis. Although the compensating regime does not enforce exact power laws, the characteristic exponents of the compensating regime are $\alpha = 3/2$ and $\alpha = 4/3$. These exponents are consistent with measurements performed in several vortices of very different scales.

References:

[1] Fujita, T.T. Tornadoes and downbursts in the context of generalized planetary scales, *J. Atmos. Sci.* **38**, 1511–1534, 1981.

[2] Einstein, H.A. and Li, H. Steady vortex flow in a real fluid, *Proc. Heat Trans. and Fluid Mech. Inst.* **4**, 33–42, 1951.

[3] Lewellen, W.S. A solution for three-dimensional vortex flows with strong circulation, *J.Fluid Mech.* **14**, 420–432, 1962.

[4] Lundgren, T.S. The vortical flow above the drain-hole in a rotating vessel, *J.Fluid Mech.* **155**, 381–412, 1985.

[5] Klimenko, A.Y. A small disturbance in the strong vortex flow, *Physics of Fluids* **13**, 1815–1818, 2001.

[6] Klimenko, A.Y. Near-axis asimptote of the bathtub-type inviscid vortical flows, *Mech. Res. Comm.* **28**, 207–212, 2001.

[7] Klimenko, A.Y. Moderately strong vorticity in a bathtub-type flow, *Theoretical and Computational Fluid Mechanics* **14**, 143–257, 2001.

[8] Shiraishi, M. and Sato, T. Switching phenomenon of a bathtub vortex, *J. Appl. Mech.* **61**, 850–854, 1994.

[9] Brooks, H.E., Doswell, C.A. and Davies-Jones, R. Environmental helocity and the maintenance and evolution of low-level mesocyclones, *Tornado: its structure, dynamics, prediction and hazards. Geophysical Monograph 79*, Amer. Geophys. Union, pp. 97–104, 1993.

[10] Dowell, D.C. and Bluestein, H.B. The 8 june 1995 McLean, Texas, storm., *Month. Weath. Rev.* **130**, 2626–2670, 2002.

[11] Wurman, J. and Gill, S. Finescale radar observations of the Dimmitt, Texas (2 June 1995) tornado, *Month. Weath. Rev.* **128**, 2135–2164, 2000.

[12] Bluestein, H.B. and Golden, J.H. Review of tornado observations, *Tornado: its structure, dynamics, prediction and hazards. Geophysical Monograph 79*, Amer. Geophys. Union, pp. 319–352, 1993.

[13] Emanuel, K. Tropical cyclones, *Annu. Rev. Earth Planet. Sci.* **31**, 75–104, 2003.

[14] Gray, W.M. Feasibility of beneficial hurricane modification by carbon dust seeding, *Atmospheric Science Paper No 196* Dept. of Atm. Sci. Colorado St. Univ., 1973.

[15] Hawkins, H.F. and Rubsam, D.T. Hurricane Hilda, 1964, *Month. Weath. Rev.* **96**, 617–636, 1968.

[16] Hawkins, H.F. and Imbembo, S.M. The structure of small intense hurricane – Inez 1966, *Month. Weath. Rev.* **104**, 418–422, 1973.